A CYLINDRICAL DRIFT CHAMBER FOR THE MEASUREMENT OF $K \to \pi\nu\bar{\nu}$ DECAY

J.V. Cresswell, S. Ahmad, E.W. Blackmore, D.A. Bryman, N. Khan, Y. Kuno and T. Numao
TRIUMF, 4004 Wesbrook Mall, Vancouver, B.C., Canada V6T 2A3

Summary

A cylindrical drift chamber has been constructed for the study of the rare kaon decay $K^+ \to \pi^+\nu\bar{\nu}$. Data from two prototype chambers and initial results from the final chamber are presented.

1. Introduction

Measurement of the $(K \to \pi\nu\bar{\nu})/(K \to \text{all})$ branching ratio provides a unique test of second-order weak interactions and is also sensitive to the existence of extra generations and other new effects. Experiment 787 at Brookhaven National Laboratory[1] aims at reaching a branching ratio sensitivity of 2×10^{-10} by using a high kaon stopping rate, a large solid angle for detection of decay particles and a high capability for background rejection.

The detector is mounted at the Low Energy Separated Beam Line I (LESB I) at BNL. The detector components are located inside a solenoid magnet. Pions from kaon decays are detected by a cylindrical drift chamber surrounding a scintillator fibre target and surrounded by stacks of scintillation counters for range and energy measurements. There are also photon veto detectors covering 4π solid angle.

The primary functions of the drift chamber, which subtends a solid angle of 50% for kaon-decay products in the range $P > 150$ MeV/c, are to provide a momentum measurement in the 1 T magnetic field and to achieve good tracking between the target and the range stack. Monte Carlo calculations indicated that a momentum resolution (rms) of 2% limited by multiple Coulomb scattering was a desirable goal for rejection of $K_{\pi 2}$ and $K_{\mu 2}$ decay-related backgrounds. Because of a high stopping rate of kaons and pions, the chamber was required to have a short memory time.

2. Design and Construction

2.1 Mechanical and cell design

The cylindrical drift chamber occupies the radial region 9.5 cm to 43.2 cm and has a total length (including the space for cables and connectors) of 65 cm. The active volume (50.8 cm in length) is enclosed by 9.5 mm thick precision-machined Aℓ endplates and graphite-epoxy cylindrical walls. The chamber is supported at the downstream endplate by a larger diameter cylinder attached to the magnet pole. The chamber is arranged in five layers of multi-sense wire cells. The wires of layers 1, 3 and 5 are axial and those of 2 and 4 are at stereo angles from 3.1° to 4.0° to enable Z position measurements. Figure 1 shows the endcap layout and side views. The drift cell geometry is shown in Fig. 2 and the drift paths followed by ionization electrons in the presence of a 1 T magnetic field are shown in Fig. 3. There are 36 to 70 cells in each layer and 256 cells in total. The sense wire plane has eight 20 μm diameter gold-plated tungsten wires spaced 5.08 mm apart. This rather narrow spacing without potential wires in the sense wire plane provides high drift fields and reduces the size of the Lorentz angle. Because of field distortions and inefficiencies caused by the Lorentz angle effect at the cell ends, only the six middle wires are instrumented. There is one additional guard wire (100 μm thick) at the end of each sense wire plane. The sense wires are staggered by 254 μm from the mid-plane to provide local resolution of the left-right ambiguity. The distance between the

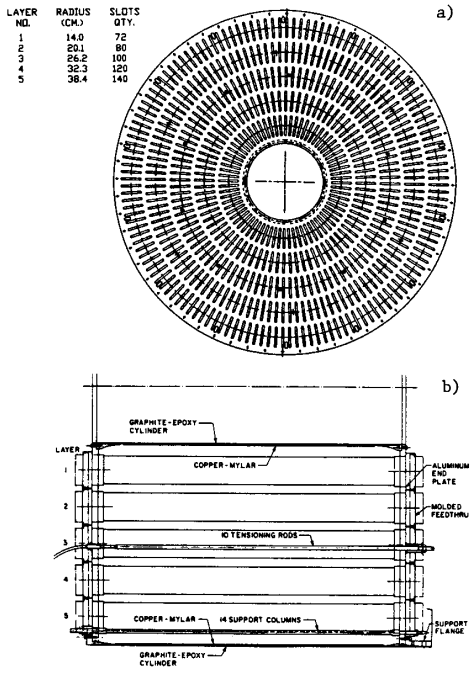

Fig. 1. (a) Drift chamber endcap layout, (b) Side view of lower half of drift chamber.

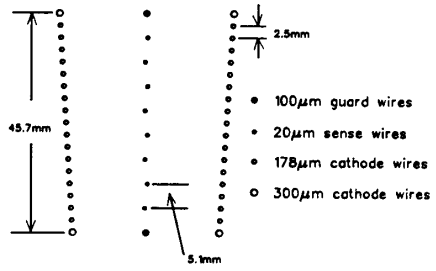

Fig. 2. Drift cell geometry (layer 3).

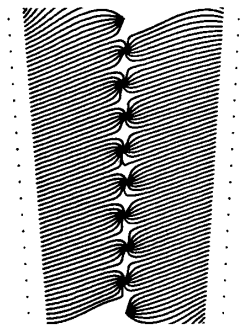

Fig. 3. Trajectories of ionization electrons in 1 T magnetic field.

0018-9499/88/0200-0460$01.00 © 1988 IEEE

sense and cathode wire planes (the half widths of the cells) vary from 1.2 cm^2 (layer 1) to 1.7 cm (layer 4). The cathode planes have 17 178 μm diameter Be-Cu wires and one 300 μm diameter Be-Cu wire at each end of the cathode plane. The surface fields of the cathode wires are kept below 25 kV/cm when those of the sense wires are around 300 kV/cm.

2.2 Construction of the final chamber

The endplates are held apart on the inner radius by a 80 mg/cm^2 thick graphite epoxy cylinder made with four preimpregnated layers arranged at 0°, 45°, 0° and -45°. To provide access for stringing the wires, the initial outer support consisted of 14 rods spaced uniformly around the outer periphery of the chamber. Due to deflection of the endplates of 0.35 mm at about half radius caused by the wire loading, initial prestressing of the endplates was done with 10 rods located in the third layer. These inner rods were removed after the chamber had been strung with three prestressing wires in each feedthrough which were later used to thread the chamber wires. The anode and cathode wires were positioned by precision grooves in Vespel combs epoxied in an injection-molded Ryton feedthrough, as shown in Fig. 4. Each feedthrough was epoxied in a slot in the endcap and carried a finger stock printed circuit board for soldering the wires. The sense and cathode wires were tensioned at 50 g and 150 g, respectively. The outer graphite-epoxy cylinder of thickness 94 mg/cm^2 was installed after all chamber wires had been strung and cleaned. When the wire load was transfered to the outer cylinder by removing the outer support rods the tensions of the outer cathode wires were adjusted to design values by shimming. The feedthroughs were then sealed with an insert card using epoxy.

2.3 Electronics and high voltage designs

The pre- and post-amplifiers were custom designed at TRIUMF. A preamplifier card contains six amplifiers based on a common-base input BFT25 transistor, as shown in Fig. 5(a). The preamplifier card is mounted on the downstream end of the sense wire plane using a printed

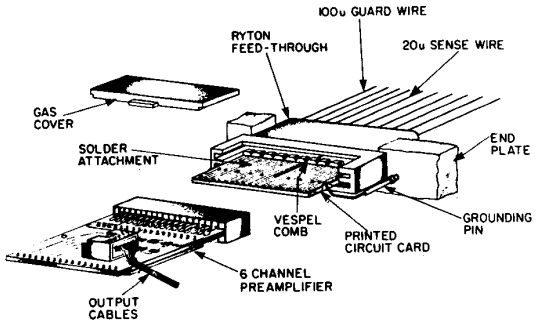

Fig. 4. Drift cell insulated feed-through showing wire positioning comb and preamplifier connections.

circuit edge connector. Each preamplifier card is grounded locally by short jumper wires to pins mounted on the endplate. A typical preamplifier gain is 10 mV/μA with a rise time of 3 ns. The power dissipation for each preamplifier is 24 mW. In order to compensate the cross-talk signals of 12-15% induced by positive ions to a level of 5%, the preamplifier has cross-talk compensation resistor chains at the front-end.

The preamplifier and the post amplifier are linked by a series of two types of 50 Ω coaxial cables: a bundle of eight 10 ft long 1.2 mm diameter ALPHA 9374 cables for each preamplifier card is used inside the magnet to the bulkhead at the downstream end of the support cylinder and an 8-way bundle of 100 ft long RG174 cables runs to the post amplifiers in the counting room. Two cables out of eight in a bundle are for ±6 V power lines to the preamplifier card. The -6 V line also carries a pulser signal for calibration. The chamber signal is attenuated approximately to half at the end of the cable and the rise time is degraded to 7 ns.

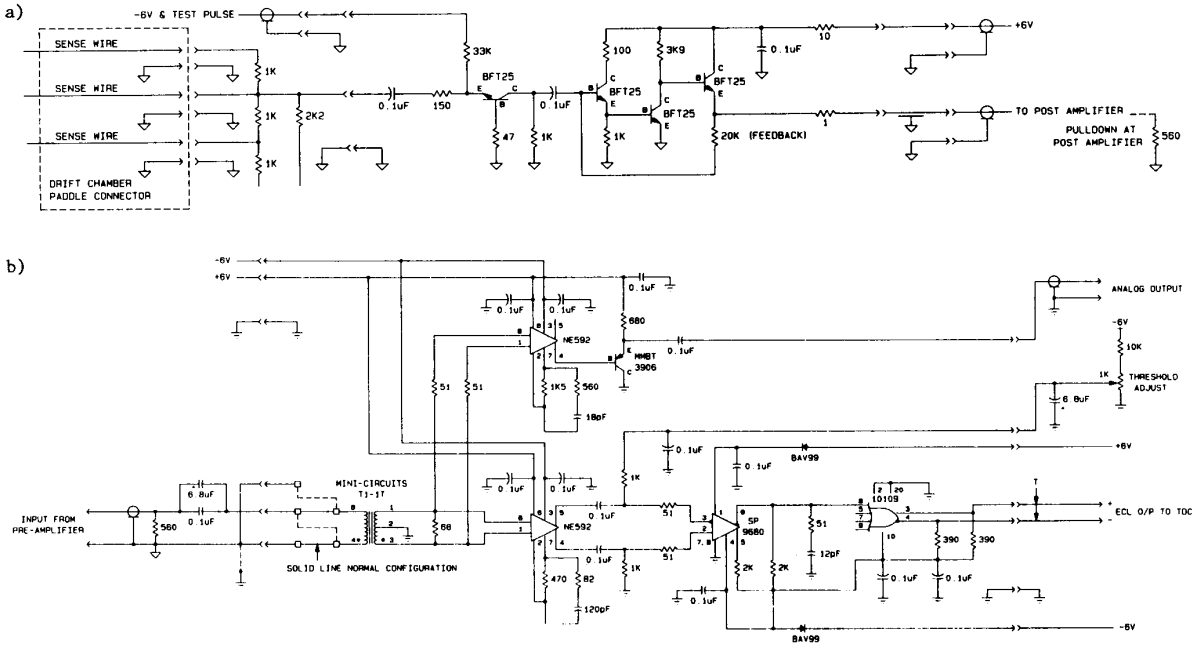

Fig. 5. (a) Preamplifier, (b) Postamplifier-discriminator.

The post-amplifier-discriminator system is housed in Euro-crates. Each post amplifier card has 24 amplifier-discriminators shown schematically in Fig. 5(b). The input signals are decoupled from ground by transformers and split into two lines, analog and discriminator paths. The gains of the amplifiers are 7-10 for the analog output and 100 for the discriminator signal path. Both amplifiers employ a pole-zero cancellation circuit and a fall time of 10 ns has been achieved. The tail of a pulse due to the positive ion movement and to the attenuation through the long cable has been reduced to a level of 2% or less. The discriminator is operated in a time-over threshold mode with a pulse stretcher to satisfy a minimum width of 10 ns required by the LeCroy fastbus TDC (model 1879).

Since all the wires in the sense planes are grounded directly or indirectly by the preamplifiers, the uniform electric field of approximately 1.7 kV/cm is provided by graded voltages on the cathode wires to meet with the variation of the cell width. A resistor-divider chain on each cathode plane at the upstream side of the chamber is connected by bus lines to adjacent cells. Each chamber layer has 3 such bus lines for the high voltage ends of resistor chains which are connected to input cables at the downstream endplate through outermost cathode wires. Corresponding three bus lines for the low voltage ends of the chains are grounded by a high-value resistor. The high voltage for each chain group is supplied by a BERTAN 1755N module and each bus line takes about 500 μA at the operating voltage. To provide the correct potentials on the inside of layer 1 and the outside of layer 5 thin copper-plated mylar foils were attached to the graphite-epoxy support cylinders and placed at the appropriate voltages.

3. Tests with prototype chambers

3.1 Prototype chambers and tests

Two prototype chambers were constructed for the initial design studies: a full-length single-cell chamber with parallel sense and cathode planes surrounded by guard wires and a 3-layer chamber with 15 tapered cells.[2] The single cell chamber was tested with ^{55}Fe and ^{106}Ru sources. Tests of the 3-layer prototype chamber were done with positive pion beams with momenta of 110-220 MeV/c from the TRIUMF M11 channel as well as with radioactive sources and cosmic rays. The momentum bite of the beam was less than 1%, and more than 95% of beam particles were pions. The chamber was placed in a magnetic field of 0.7 T. The 3-layer prototype chamber was also used to study the resolution along the wire by re-stringing wires in the second layer at angles of 2.3°. Two MWPC chambers were placed at the top and bottom of the prototype chamber to identify cosmic-ray tracks independently.

Three gas mixtures, $Ar(89)+CO_2(10)+CH_4(1)$, $Ar(90)+CH_4(10)$ and $Ar(50)+C_2H_6(50)$ with alcohol, were tested in the single cell prototype chamber. Because of gas stability, a wider plateau and better position resolution, the mixture $Ar(50)+C_2H_6(50)$+alcohol was used throughout the tests and is used in the final chamber.

3.2 Data analyses

Parameters for the present cell design, such as the drift velocity and the Lorentz angle, were studied by fitting tracks. The drift time is converted into a local co-ordinate in a cell and also into a global co-ordinate using a given drift velocity and Lorentz angle after pedestal subtraction. Track segments are sought in a cell throughout the chamber using the road method and are translated into a vector, which is used in the next step. Combinations of track segments are then examined for the validity of being on the same track in order to form a track. Good points within deviation limits from the fitted trajectory are kept in the subsequent iteration process. Some corrections such as wire-crossing angle corrections are then applied and track parameters are calculated again.

3.3 Results of the prototype tests

The drift velocity was determined by fitting tracks which cross the cell boundaries. In order to avoid field distortion effects in the neighborhood of the wires, data points close to the cathode wire plane were omitted from the fit. Local chi-squared was minimized in a layer to obtain the drift velocity for each layer. The measured drift velocity was 5.1 cm/μs. If data are taken under a magnetic field, the Lorentz angle is another parameter to be determined from the local chi-squared. The minimum chi-squared was sought in the two dimensional map of drift velocity and Lorentz angle. The extrapolated values from the data at 0.4-0.7 T give $\alpha = 25\pm5°$ for 1 T, assuming $\alpha = 0°$ at 0 T.

Dependence of the position resolution on the drift distance was obtained from the residual of the fit. Using preamplifiers not compensated for cross talk the position resolutions were estimated to be 170 μm from the deviation of the track fit (this was further improved by 20% with the addition of cross-talk cancellation resistor chains). The intrinsic chamber resolution was estimated to be around 100 μm from the position dependence of the resolution. The (rms) width of the residual distribution in the Z direction was found from the single stereo layer to be about 4 mm.

The peak position in the momentum spectra of pions was in good agreement with the incident beam momentum 200 MeV/c, indicating that there were no major systematic problems. The resolution (rms) was 7%. Using expected improvement factors for the final chamber such as the track length in the chamber and the number of points, the projected momentum resolution was estimated to be 1.3%. The estimated contribution to the momentum resolution from the position determination error is expected to be less than that from multiple scattering in the chamber gas.

Using drift distances of three adjacent wires and their relation for a local resolution, $R = X_n - (X_{n+1}+X_{n-1})/2$, the staggering distance as a function of the wire position Z was obtained from the position shift of double peaks in the histogram of R. A quadratic dependence of the deviations from 254 μm was observed with a maximum deviation of 15 μm at the middle of a wire. The size of the deviation was consistent with wire deflection due to electrostatic effects.

A section of the chamber (4×4 cm^2) was exposed to a high rate beam of 5×10^5 pions/s. Although the track reconstruction efficiency dropped slightly by 1% when the rate went up, the position resolution was not affected. Aging effects were studied with the single cell chamber by exposing it to a high intensity radioactive source. No significant effects within a 10% measurement error were observed up to the total charge 0.1 C/wire/cm.

4. Initial Results from the Final Chamber

The final chamber assembly was tested at TRIUMF with sources and cosmic rays. Initially, there were two high voltage related problems. One was a noise problem from high voltage discharge outside the chamber due to humidity. This problem was eliminated after the installation of a dry-air bag. The other one was possibly

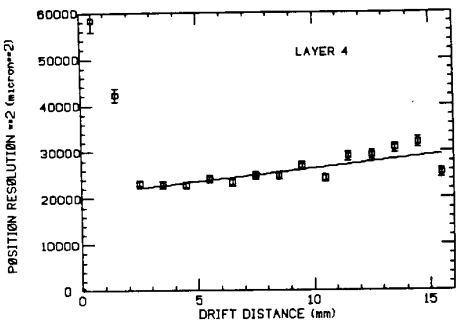

Fig. 6. Resolution vs. drift distance (layer 5) with a fit to $\sigma^2 = \sigma_o^2 + D^2x$.

due to some sharp-pointed objects such as dust particles and uncleaned flux on chamber wires. This problem required about a week of voltage conditioning eventually up to the operational voltages and some 'back-biasing' with reversed polarity high voltage up to the half of the operational values.

All results from the initial tests were consistent with the prototype study. The position resolution was obtained to be an average value of 150 μm using the three-adjacent-wire technique. Figure 6 shows the variation of position resolution with drift distance for a cell in layer 4. The data are fitted to the form $\sigma^2 = \sigma_o^2 + D^2x$ where the slope D represents the effects due to diffusion. For this data we find D=76±3 μm/$\sqrt{\text{cm}}$. The distance between staggered sense wires agrees with the design values of 254 μm within 5%. The variation was about 30 μm. The efficiencies of the wires were found to be better than 98%. The Z position resolution was also studied by examining the residual distibution of each hit from Z fitting, showing a preliminary rms value of 2.5 mm.

References

[1] BNL experiment 787. BNL, Princeton University, TRIUMF collaboration.
[2] S. Ahmad et al., IEEE Trans. NS-33, 178 (1986).